Available online at www.sciencedirect.com
SCIENCE DIRECT®
Polymer 45 (2004) 3351–3358
polymer
www.elsevier.com/locate/polymer

Crosslink densities and phase morphologies in thermoplastic vulcanizates

Maria D. Ellul[a], Andy H. Tsou[b,*], Weiguo Hu[b]

[a]*Advanced Elastomer Systems, Akron, OH 44311, USA*
[b]*Baytown Technology and Engineering Complex - West, ExxonMobil Chemical Company, 5200 Bayway Drive, Baytown, TX 77520, USA*

Received 14 December 2003; received in revised form 7 March 2004; accepted 9 March 2004

Abstract

The degree of EPDM crosslinking during dynamic vulcanization of a PP/ EPDM thermoplastic vulcanizate (TPV) was modified by varying its phenolic curative content. The rise in TPV viscosity, the drop in its swelling, the change in its NMR MAS lineshape, and the increase in its EPDM domain AFM force modulation hardness verified the increase in EPDM crosslink density with increasing curative content. Further, the EPDM crosslink extent in TPV was measured by either the bound phenolic or the residual diene content both determined by solid state NMR. SEM morphologies of cryo-faced and ruthenium-stained TPVs with varying curative contents were analyzed to determine the effects of cure on EPDM domain sizes and PP ligament thickness. A narrowing of the EPDM domain size distribution, with a decrease in the third moment of the distribution, was observed with increasing EPDM crosslink density. Correspondingly, the PP ligament number-average thickness was raised slightly.

Keywords: TPV; Dynamic vulcanization; EPDM

1. Introduction

Thermoplastic vulcanizates, or TPVs, are blends where the elastomer component is vulcanized in situ during melt mixing with the thermoplastic component at high shear and elevated temperature. Dynamic vulcanization of the elastomer component in a TPV enables the crosslinked elastomer, or rubber, to become the dispersed phase even in cases where the elastomer is the majority component, or its volume fraction is greater than 0.5. This raised elastomer viscosity through vulcanization affects the phase continuity and promotes the phase inversion, i.e. the majority phase becomes the dispersed phase [1–3]. Additionally, the thermoplastic component, despite being the minority phase, remains the continuous phase and, thus, preserves the ease of processing of thermoplastics. High rubber volume concentrations are required for the resulting TPV to behave elastomerically. Besides ensuring the thermoplastic phase continuity, crosslinks introduced during dynamic vulcanization also lower the tension set and raise the tensile strength [4] of the TPV.

Ultimate elongation and tensile strength of a TPV depend upon both the crosslink concentration in the rubber phase and its dispersion morphology, in terms of the rubber domain sizes and distributions [4]. Considering that the degree of crosslinking in the rubber phase could have profound effects on its viscosity and elasticity during mixing with the thermoplastic, changes in rubber domain morphology are expected in TPVs with vary curative contents. In this study, the curative concentration in EPDM in an EPDM/PP TPV is varied. The corresponding increase in effective crosslink density with curative content in these TPVs was confirmed by solvent swelling, viscosity, NMR signal line width, bound curative content, residual diene concentration, and domain hardness measurements. Effects of crosslink density on phase morphology in these TPVs were evaluated based on image processing [5] of SEM micrographs of ruthenium tetraoxide stained and cryo-faced TPV samples with varying crosslink density.

2. Experimental

2.1. Materials

TPV materials used in this study consisted of EPDM, polypropylene (PP), process oil, mineral filler, and phenolic

* Corresponding author. Tel.: +1-281-8342823; fax: +1-281-8342920.
E-mail address: andy.h.tsou@exxonmobil.com (A.H. Tsou).

0032-3861/$ - see front matter © 2004 Published by Elsevier Ltd.
doi:10.1016/j.polymer.2004.03.029

resin curative. They were prepared by dynamic vulcanization using an intermeshing twin screw extruder. In this process, the EPDM elastomer was vulcanized in situ into rubber during melt mixing with the thermoplastic at 200 °C. The result was a micron-sized dispersion of crosslinked EPDM rubber particles in a thermoplastic PP matrix with paraffinic process oil solubilized in both the rubber and the amorphous polypropylene fraction [6]. The absolute contents of EPDM, PP, filler, and oil were kept constant in this study only with the phenolic resin curative varied according to Table 1. The soft TPVs listed in Table 1 have 30 wt% EPDM, 14 wt% PP, 42 wt% process oil, and 12 wt% mineral filler when 2 wt% curative was used.

Similar thermoset rubber samples (TS), similar in composition to that of the soft TPVs, were also made. These rubber samples contained 42% process oil but without any PP. They were cured at 200 °C to 90% completion (controlled by the cure time), as measured by a moving die rheometer. Curative levels in these TS samples are shown in Table 2. Both TS rubbers and soft TPVs were extracted in acetone/cyclohexane (2:1) azeotrope to remove process oil in order to determine if the presence of the process oil could have affected the NMR results.

A second set of TPVs, which were PP-rich, were made. These TPVs are called Hard TPVs in this study. They have 20 wt% EPDM, 44 wt% PP, 25 wt% process oil, and 10 wt% mineral filler when 1 wt% of phenolic curative was used. Their Shore D hardness values were around 40 (Table 3).

2.2. Mechanical, swelling, and rheological properties

Stress–strain properties of these TPVs were measured on 2 mm thick injection-molded ISO-standard plaques at 23 °C according to ASTM D-142 and their tension set values were obtained at the same temperature per ASTM D-142. Samples were die cut in the long direction. After soaking these TPVs in IRM No. 3 fluid for 24 h at 125 °C, their weight gains, or swellings, were determined according to ASTM D-471. Automatic Capillary Rheometer (ACR) viscosity, which is a measure of the TPV shear viscosity at a fixed shear stress of 118 kPa, was measured for these TPVs at 204 °C. The capillary used has a 33/1 L/D ratio and a 0.78 mm diameter orifice. The shear rate applied in this capillary test is at 3000 1/s. Additionally, their complex viscosity values at 200 °C were evaluated using a Rheometrics RDA II instrument with circular discs in a frequency sweep mode.

Table 1
Soft TPV compositions (with about 65 Shore A Durometer hardness)

Sample ID	Curative content (wt%)
TPV-1	0.6
TPV-2	1.4
TPV-3	2.2

Table 2
Thermoset compositions

Sample identification	Curative content (wt%)
TS-1	1.7
TS-2	0.7
TS-3	1.7
TS-4	2.7
TS-5 (uncured reference)	0

2.3. Solid state NMR

Instead of characterizing the crosslink density using swollen TPVs via solution ^{13}C NMR [7], solid state ^{1}H NMR is applied directly in this study. Solid state NMR experiments were performed on both as-received TPVs as well as on the extracted TPVs using a Bruker DSX-500 spectrometer with 500.13 MHz ^{1}H frequency and 125.75 MHz ^{13}C frequency. All samples were tested on a 4 mm rotor at a 5-kHz spinning speed controlled by a two-second recycle delay. The magic angle spinning, or MAS, was utilized where the angle between the spinning axis and magnetic field is 54.7°. Since segmental mobility increases with temperature, it is desirable to run NMR experiments at elevated temperatures for better resolution. In this study, one-pulse ^{1}H spectra were acquired both at room temperature and at 80 °C for each sample.

2.4. SEM morphology

Broad rubber dispersion size distributions and large rubber dispersions were observed in these TPVs. Considering that the variance of image processing is inversely proportional to the square root of the feature count [5], lower-magnification SEM, at 500 to 1500 X, was employed in this study for higher feature counts, i.e. more observable rubber dispersed domains in a given image. In order to provide electron density contrast between PP and EPDM in these TPVs, ruthenium staining was required. All TPV samples were cryo-faced at − 150 °C, using a diamond knife and a Reichert cryogenic microtome, to prepare fresh and flat surfaces prior to uniform staining by ruthenium vapor for 2.5 h. Subsequently, cold facing at − 20 °C was performed to remove potentially over-stained surface layers for better contrast. SEM images were taken by a JSM-5600 LV SEM at 10 keV. All acquired SEM images were

Table 3
Hard TPV compositions

Sample identification	Curative content (wt%)
TPV-6	0.5
TPV-7	1.2
TPV-8	1.6

converted to TIFF format and processed using PHOTOSHOP® (Adobe Systems, Inc.) for image enhancement. An image processing tool kit from Reindeer Games was applied for image measurements, results of which were then written into a text file for EXCEL® (Microsoft) data processing to compute dispersion sizes. Horizontal and vertical lines that are 1 pixel in width and 1 pixel apart were also overlaid on the thresholded binary TPV images to measure the lengths and widths of the continuous phase, or PP domain. Results of these image-processing measurements are used for the determination the PP ligament thickness.

2.5. Force modulation AFM

The AFM measurements were performed in air and at room temperature on a NanoScope Dimension 3000 scanning probe microscope (Digital Instrument) using a rectangular 225 μm Si cantilever on cryo-faced TPV samples. These TPV specimens were cryo-faced at −150 °C with diamond knives in a Reichert cryogenic microtome and, then, stored in a dessicator under flowing dry nitrogen to prevent surface condensation. The stiffness of the cantilever used is ~4 N/m with a resonance frequency of ~70 kHz. The free vibration amplitude at resonance is high, ranging from 80 to 100 nm, with a RMS setting of 3.8 V. The set point ratio was maintained at or lower than 0.5 during each tapping AFM measurement to ensure repulsive contacts with positive phase shifts [8–11]. During tapping, the cantilever was running at or slightly below its resonance frequency [12]. The topology of the sample was first mapped using the tapping mode prior to the application of force modulation. During force modulation, the cantilever tip was lowered by a specified 50 nm from the surface defined by tapping. The cantilever was then oscillated in its indentation mode at the bimorph resonant frequency of ~10 kHz. During scanning, drive amplitude for the bimorph-driven force modulation was set at 500 mV and response RMS amplitudes of the cantilever were measured. Bimorph driven force modulation is a displacement modulation with reference to the tip holder [13]. However, without the knowledge of the input tip amplitude (only the drive amplitude for the bimorph is known), the mechanical modulus of the sample cannot be calculated from the response amplitude. Instead, relative difference in response RMS amplitude between the EPDM and PP in a given sample was measured, in this study, for comparison of EPDM hardness between TPVs with varying curative contents. High variability was observed during tapping phase and force modulation measurements of TPV samples without extraction. The variability is attributed to the non-uniform presence of process oil. All results reported here are based on AFM measurements on extracted TPV samples.

3. Results and discussion

3.1. Crosslink density

As shown in Fig. 1, the effect of curative level on stiffness of the EPDM rubber phase can be first observed on 'equivalent' thermoset EPDM vulcanizates according to torques measured using a Moving Die Rheometer ($(S'_{max} - S'_{min})$ in Fig. 1). It should be pointed out that this is a static vulcanization in the absence of PP thermoplastic component and high shear mixing environment. It is not a one-to-one equivalence to dynamic vulcanization due to the lack of high shear that can translate to a different curative efficiency. The purpose of this measurement is to demonstrate the differences in stiffness that can be obtained by varying the curative level from 0.7 to 2.7%. The peak rate shown in Fig. 1 is the maximum torque increase rate and is a measure of the static vulcanization rate that, again, is different from the dynamic vulcanization rate obtained during the preparation of TPV. The corresponding physical crosslink density range determined according to uniaxial stress strain measurements of these thermosets is around 20–100 mol/m^3.

The relative modulus or degree of crosslinking of the rubber phase in a TPV could be estimated from the elastic storage modulus, G', of the TPV at elevated temperatures, above the melting of the thermoplastic component, in the linear viscoelastic regime. An increase in storage modulus in soft TPVs with curative content is indicated based on the oscillatory shear measurement results, as shown in Fig. 2, at 200 °C. Additionally, the crosslink density of the EPDM rubber has a major effect on swelling and recovery properties of the TPV as exhibited in Fig. 3. Both the tension set and fluid resistance as measured by swelling in IRM No. 3 fluid can be improved by a factor of about two over the curative concentration range of 0.6–2.2%. The capillary viscosity of the TPV can also be raised significant by the cure state of the EPDM phase, especially at high shear rates where the viscosity of the thermoplastic component is low, as shown in Fig. 4.

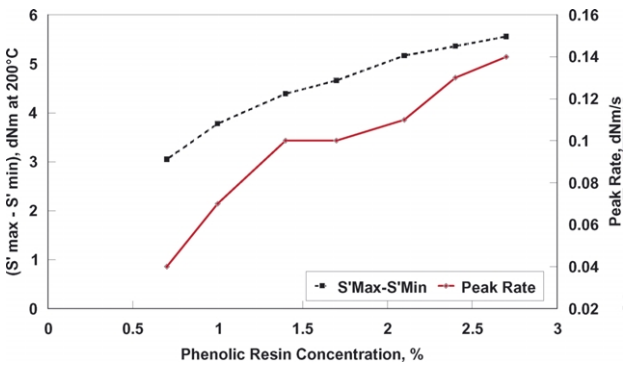

Fig. 1. Effect of phenolic resin concentraion on MDR torque and cure rate at 200 °C of EPDM vulcanizates, or TSs.

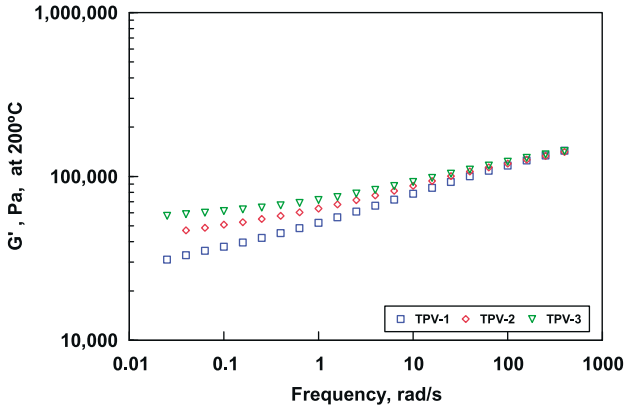

Fig. 2. Effect of curative level on elastic modulus, G', at 200 °C.

3.2. Crosslink density by SSNMR

^{1}H one-pulse SSNMR spectra were acquired and analyzed to determine the crosslink extents in these TPVs. A representative spectrum is shown in Fig. 5. Signals originating from methyl, methylene, residual diene, and aromatic components can be seen. There are three parts within each spectrum that can be used to estimate the curing extent in a TPV and they are:

3.2.1. Backbone peak base width

Signal width of a given polymer segment is directly related to its mobility. A reduction in segmental mobility results in a broadened segment signal. In cured systems, segments close to a crosslink are less mobile than segments that are away. Since close-to-crosslink segments have wider signal line width as compared to that obtained from away-from-crosslink segments, they contribute more to the base of the peak. On the other hand, the away-from-crosslink segments, or non-crosslinked linear segments, contribute more to the narrower part of the peak. In this study, the line width at peak base (< 1% of maximum) is used as a measure of the crosslink density. Peak widths at 50% maximum are similar among the three soft TPVs and among the five TS

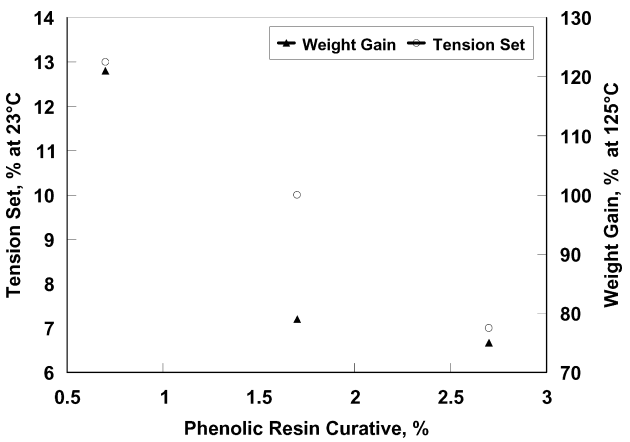

Fig. 3. Effect of phenolic resin concentration on swelling in IRM No. 3 fluid and tension set of TPV.

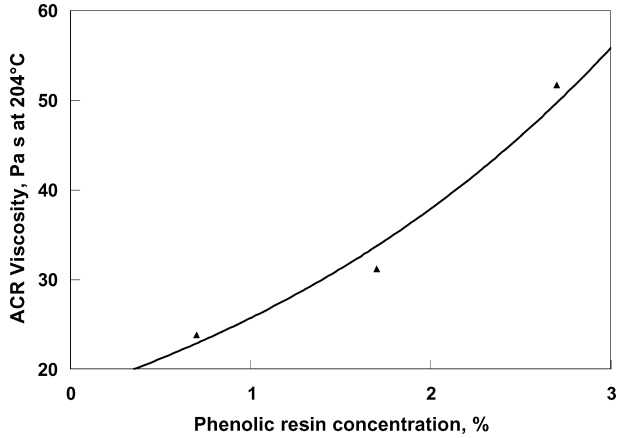

Fig. 4. Effect of cure state on capillary viscosity of TPVs.

thermoset samples evaluated, but their peak base widths are quite different as shown in Fig. 6. For the EPDM thermoset TS samples, peak widths selected at 0.2, 0.5, and 1.0% of maximum measured at room temperature as a function of curative content are plotted in Fig. 7. All three selected measures are sensitive to the curative content. Linear correlation coefficient squares for all three measures are between 0.95 and 0.96.

In order to understand the underlying mechanism for the peak broadening at the signal base with increasing crosslink density, ^{1}H MAS experiments were conducted on extracted TS1-5 thermoset samples at 80 °C. It was found that the ^{1}H MAS line widths at 1% maximum does not correlate to the curative content at 80 °C. Considering that T_2 relaxation difference generally persists at elevated temperatures, this peak base broadening is probably not related to T_2 relaxation. On the other hand, residual ^{1}H–^{1}H dipolar coupling decreases at higher temperatures that could lead to the observed disappearance of the correlation and, thus, is most likely responsible for MAS peak base broadening.

Crosslinking extents in rubbers have been extensively studied using solid state NMR in the literature [14–16] mostly based on relaxation evaluations of non-spinning samples. The relationship between cure state of a rubber and its MAS lineshape has not been established. Despite the NMR signal contributions from the protonated process oil, a strong correlation between crosslinking and MAS lineshape in unextracted TPVs was still obtained in this study. However, considering that that the ^{1}H NMR linewidth can be affected by other factors, other than the crosslink, using this MAS lineshape method for cure state measurement should be applied with caution. The presence of polypropylene, strong interactions between polymer and fillers, and the magnetic field inhomogeneity could all broaden the peak base width. In addition, spectrometer conditions must be kept the same and experiments need to be done using the same shimming parameters.

3.2.2. Aromatic content

The aromatic protons in the curative resonate at ~7 ppm,

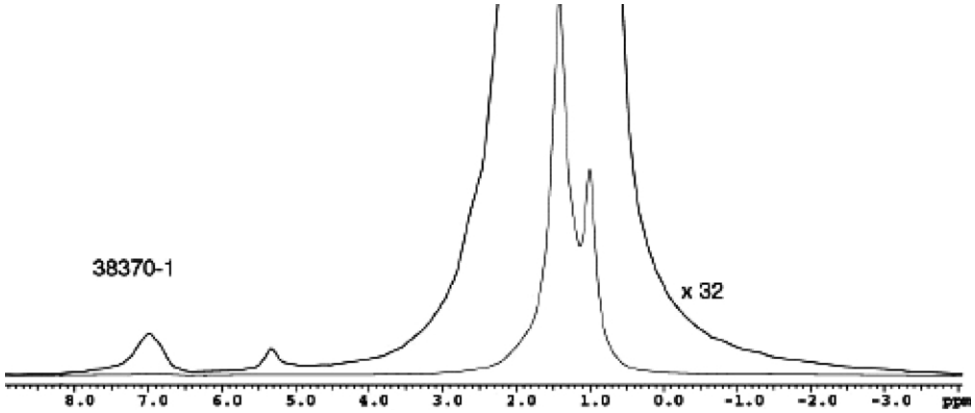

Fig. 5. ^{1}H MAS NMR spectrum of thermoset TS-1 (before extraction). The upper trace is the same spectrum as the lower trace, but with an amplification factor of 32. The spectrum was collected at room temperature. Signals at 1.0, 1.4, 5.1–5.3, and 7.0 ppm represent methyl, methylene, residual diene, and aromatic components, respectively.

which can be clearly seen in the ^{1}H spectra (as indicated in Figs. 5 and 6). These aromatic protons could be on either phenolic molecules that are part of the crosslinks, or unreacted phenolic, or aromatic components in the process oil. After extraction to remove unreacted curative and process oil, the signal at 7 ppm in extracted TPV samples could only come from the bound phenolic. In Fig. 8, ^{1}H spectra of two extracted TS thermoset samples are shown. These experiments were performed at 80 °C for better spectra resolution. The ratio of aromatic area (~7 ppm) to the total area under the backbone peaks, including EPDM backbone and a small portion of mobile amorphous component in PP, was calculated. This aromatic area ratio is a function of the curative content for both TS and TPV samples as shown in Fig. 9(A). A strong correlation between the curative concentration and the aromatic area ratio suggests that the bound phenolic content can be used as a measure of the crosslink density.

3.2.3. Diene content

Several mechanisms for phenolic cure of diene have been proposed [17,18]. The 1,4-cyclic addition mechanism suggested that dienes are consumed during cure leading to a saturated backbone [17]. Representative ^{1}H spectra of two extracted TS samples are shown in Fig. 8. The peaks at 5.1 and 5.3 ppm are assigned to the two isomers of ENB, ethylene norborene, unsaturated protons, respectively. There is also a small 9.7 ppm peak which could be related to certain acidic protons generated during cure. As shown in Figs. 8 and 9(B), a reduction in diene content is indicated with increasing curative content suggesting the consumption of diene with cure.

However, according to one of the other proposed mechanism [18], the diene that has reacted with curative on the allylic hydrogen position could have preserved the unsaturation. In that case, residual dienes in a cured EPDM could have come from two possible sources with one being

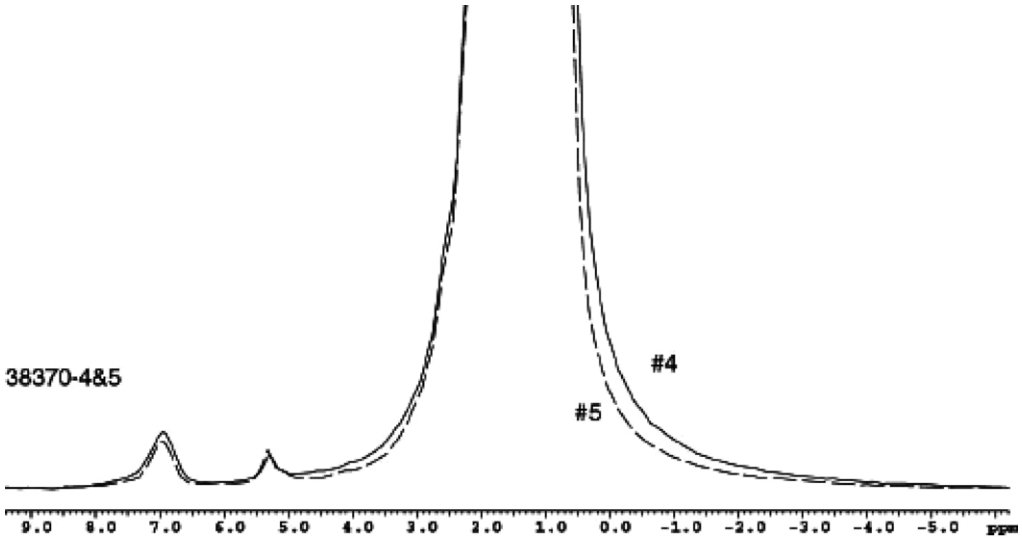

Fig. 6. ^{1}H MAS NMR spectrum of thermoset TS-4 and thermoset TS-5 (uncured reference) before extraction. The spectra were acquired at room temperature.

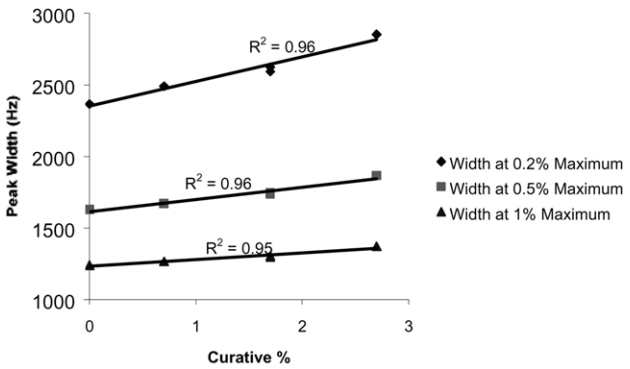

Fig. 7. ^{1}H MAS NMR backbone peak base width of EPDM thermosets before extraction as a function of curative content. The ^{1}H spectra were acquired at room temperature.

the unreacted diene. Fortunately, these two types of unsaturation can be differentiated on the basis of their different dynamic behavior. The unreacted diene would have had much more motions than that of reacted diene due to the crosslink structure. As a result, the latter would have had presumably a much shorter ^{1}H T_2. Our NMR results indicated that all diene signals have a slightly longer ^{1}H T_2 than that of the backbone ruling out this proposed mechanism of retaining unsaturation during cure. It should be pointed out that the extrapolations in Fig. 9(B) lead to different ENB contents without curative for TPV and for TS samples. However, considering that the normalization of measured NMR diene content involves using the total area under the polymer backbone, which is different between TPV and TS, this difference is expected. The normalization area for TPVs includes EPDM backbone and a small portion of mobile amorphous component in PP whereas that for TSs contains only EPDM.

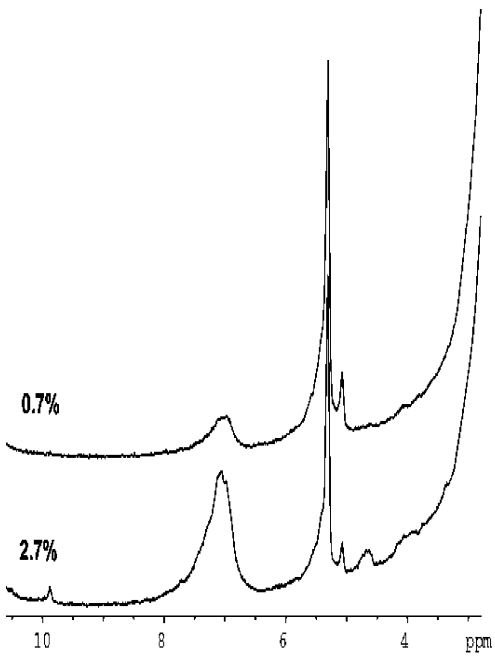

Fig. 8. ^{1}H MAS spectra of EPDM thermoset samples (after extraction), with % phenolic resin curative content indicated. Spectra were acquired at 80 °C.

3.3. Crosslink density by force modulation AFM

Constant amplitude is maintained in tapping-mode AFM. Changes in phase angle, or phase lag, during tapping across a specimen resulting from tip-sample interactions are acquired and, in turn, provide tapping phase images. This phase-shift contrast, i.e. differences in phase lag, is associated with mechanical property variations in the presence of conservative and dissipative interactions. Without any energy dissipations in tapping, phase shift change is proportional to the contact area multiplied by the effective modulus [11]. Dissipative energy losses, such as adhesion hysteresis and/or viscous damping, modify the relationship between phase shift change and material modulus. Numerical simulations [19,20] and analytical approximation [21] of nonlinear dynamic behavior of an oscillating tip-cantilever system in the tapping mode determined that the relationship between phase shift change and modulus is energy-loss dependent. In this study, phase shift differences between EPDM and PP were measured in each sample. No correlation could be found between the

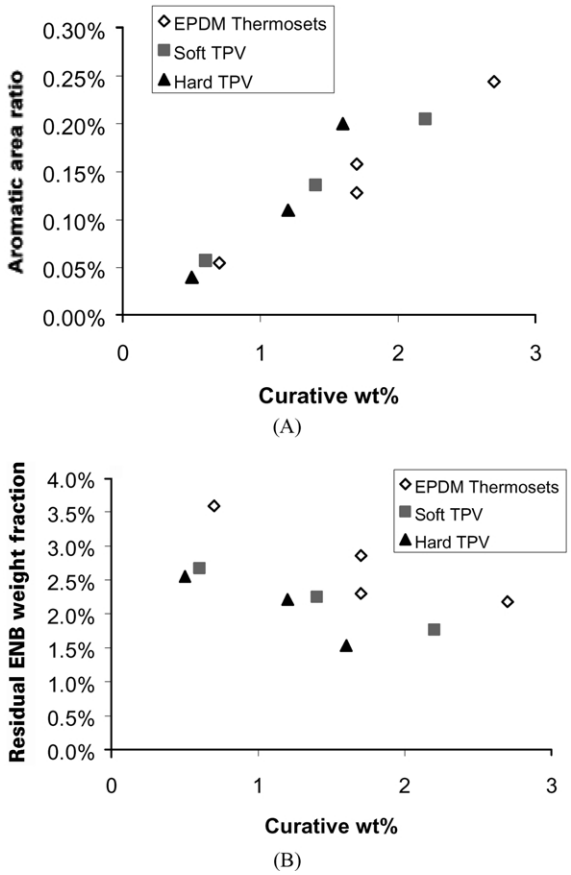

Fig. 9. Bound curative (A) and residual diene contents (B) of EPDM thermosets and TPVs (after extraction) as a function of the curative content. Spectra were acquired at 80 °C.

phase shift difference and curative content in the three soft TPVs evaluated. This lack of correlation may arise from the facts that there are other energy dissipation processes, beyond the mechanical damping, present in the tapping phase measurements of these samples.

Force modulation amplitude differences in EPDM between the three soft TPVs evaluated were found, instead, to correlate with the curative content. As shown in Table 4, increase in force modulation amplitude was observed with increasing curative content. The force modulation amplitude is a measure of the mechanical stiffness of the sample without the interference of other energy loss processes, such as the adhesion hysteresis, despite the fact that the relationship between the force modulation amplitude and modulus is complex. Using the increase in force modulation amplitude as a measure of the increase in crosslink density has been previously demonstrated in NR [22] and more recently in SBR [23]. Our results extend the application of using force modulation AFM to measure the crosslink density variations of EPDM in a dynamically vulcanized TPV.

3.4. Morphology by SEM

A representative SEM micrograph of TPV-1 is shown in Fig. 10 where the light phase is EPDM, the dark phase is PP, and the bright areas are electron-charging artifacts. Using image processing for phase separation and for removal of charging artifacts, SEM images of all three soft TPV samples were analyzed and their EPDM dispersion size distributions are plotted in Fig. 11. First to third moments of the EPDM domain size distributions are listed in Table 5. Based on Fig. 11 and Table 5, it is clear that an increase in curative content reduces the population of large dispersions. This, in turn, leads to narrower doamin size distributions at the high domain size tail of the distribution and smaller values in the higher moments of the distribution. PP continuous phase widths and lengths were also measured. Their number averages are listed in Table 5 and are shown to increase with curative content coinciding with the narrowing of EPDM domain size distribution. According to the TPV deformation mechanism proposed by Boyce et al. [24,25], thinner PP ligaments and their abilities to yield, bend, rotate, and buckle are critical for the development of pseudo-elastic network and the elasticity in TPV. Considering that an increase in curative content could lead to the thickening of PP ligament, there is an upper limit for the amount of curative that can be added in a TPV without compromising its elastic properties.

Table 4
Force modulation RMS amplitude of EPDM with reference to PP

Sample ID	Curative content (%)	Force modulation amplitude (nm)
TPV-1	0.6	2.096[a]
TPV-2	1.4	3.621
TPV-3	2.2	4.898

[a] Standard deviation of the measurement is around 0.15 nm.

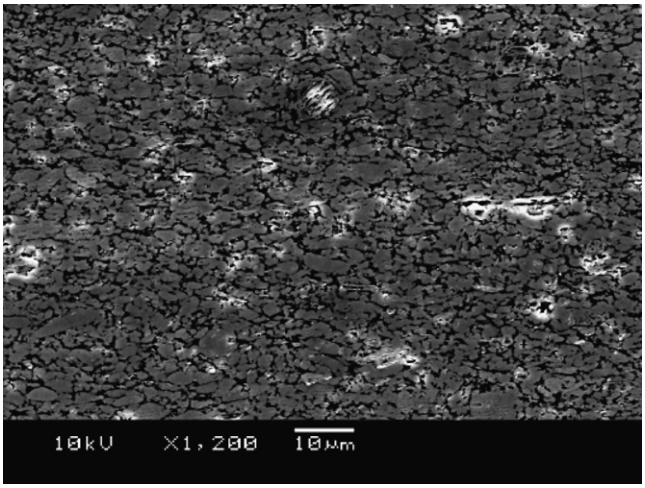

Fig. 10. SEM micrograph of TPV-1 with 0.6% curative.

4. Conclusions

During dynamic vulcanization of a PP/EPDM TPV, cure extents in its EPDM dispersions were modified by varying the phenolic curative content. The rise in TPV viscosity, the drop in its swelling, and the increase in its dynamic modulus indicated an increase in EPDM crosslink density with curative content. Using either backbone peak base width, bound aromatic curative content, or residual diene concentration, SSNMR was demonstrated to be a useful tool in direct measurement of crosslink density in TPV. Although no correlation could be found between the phase shift difference and curative content in TPVs evaluated using tapping-phase AFM, the AFM force modulation amplitude of EPDM domain with reference to PP was found to correlate with the curative content. SEM morphologies of cryo-faced and ruthenium-stained TPVs were quantified by image processing. A narrowing of the EPDM domain size

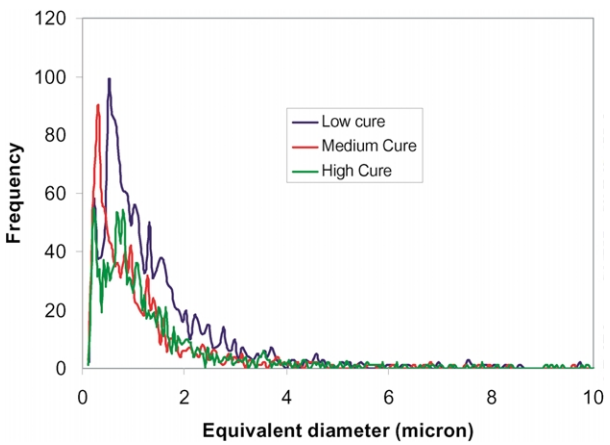

Fig. 11. EPDM particle size distributions in TPV-1, TPV-2 and TPV-3.

Table 5
EPDM domain size distribution moments and PP continuous phase sizes in TPVs

Sample	Curative (%)	EPDM first moment (micron)	EPDM second moment (micron)	EPDM third moment (micron)	PP phase size (micron)
TPV-1	0.6	1.404	2.996	6.473	0.625
TPV-2	1.4	1.130	2.742	5.808	0.726
TPV-3	2.2	1.333	2.834	5.010	0.731

distribution, with a resulting decrease in the third moment of the domain size, was observed with an increase in crosslink density. In addition, the PP ligament thickness number average was raised with increasing cure.

Acknowledgements

One of us, M.D. Ellul, would like to thank Jeff White for his initial solid state NMR work on evaluating crosslink density in peroxide-cured EPDM/PP TPVs. We would like to acknowledge experimental assistance from C. Hrbacek, R. Griffith, J. Gorsuch, Sunny Jacob, Connie Qian, Jerry Ball, Joyce Cox, and Margaret Ynostroza. The authors would like to thank Advanced Elastomer Systems, L.P. and ExxonMobil Chemical Company for their permission to publish this work.

References

[1] Paul DR, Barlow JW. J Macromol Sci, Rev Macromol Chem 1980; C18:109.
[2] Metelkin VI, Blekht VS. Kolloid Zh 1984;46:476.
[3] Ultracki LA. J Rheol 1991;35:1615.
[4] Coran AY, Patel RP. Thermoplastic elastomers based on dynamically vulcanized elastomer–thermoplastic blends. In: Holden G, Legge NR, Quirk R, Schroeder HE, editors. Thermoplastic elastomers, 2nd ed. New York: Hanser; 1996. p. 153. Chapter 7.
[5] Russ JC. The image processing handbook, 2nd ed. Boca Raton: CRC Press; 1994.
[6] Ellul MD. Rubber Chem Technol 1998;71:244.
[7] Ellul MD, Patel J, Tinker AJ. Rubber Chem Technol 1995;68:573.
[8] Magonov SN, Elings V, Whangbo M-H. Surf Sci 1997;375:L385.
[9] Kruger D, Anczykowski B, Fuch H. Ann Physik 1997;6:341.
[10] Garcia R, Tamayo J, San Paulo A. Surf Interface Anal 1999;27: 312.
[11] Spatz JP, Sheiko S, Moller M, Winkler RG, Reineker P, Marti O. Nanotechnology 1995;6:40.
[12] Burnham NA, Gremaud G, Kulik AJ, Gallo P-J, Oulevey F. J Vac Sci Technol, B 1996;14:1308.
[13] Kruger D, Anczykowski B, Fuch H. Ann Physik 1997;6:341.
[14] Simon G, Baumann K, Gronski W. Macromolecules 1992;25:3624.
[15] Litvinov VM, Barendswaard W, van Duin M. Rubber Chem Technol 1998;71:105.
[16] Leisen J, Breidt J, Kelm J. Rubber Chem Technol 1999;72:1.
[17] Lattimer RP, Kinsey RA, Layer RW, Rhee CK. Rubber Chem Technol 1989;62:107.
[18] van Duin M, Souphanthong A. Rubber Chem Technol 1995;68:717.
[19] Tamayo J, Garcia R. Appl Phys Lett 1997;71:2394.
[20] Anczykowski B, Kruger D, Babcock KL, Fuch H. Ultramicroscopy 1996;66:251.
[21] Wang L. Appl Phys Lett 1998;73:3781.
[22] Galuska AA, Poulter RR, McElrath KO. Surf Interface Anal 1997;25: 418.
[23] Mareanukroh M, Eby RK, Scavuzzo RJ, Hamed G. Rubber Chem Technol 2000;73:912.
[24] Boyce MC, Kear K, Socrate S, Shaw K. J Mech Phys Solids 2001;49: 1073.
[25] Boyce MC, Socrate S, Kear K, Yeh O, Shaw K. J Mech Phys Solids 2001;49:1323.